Received: 04.04.2026 | Revision: 26.05.2026 | Accepted: 28.05.2026 | Published: 12.09.2026

Veterinary Sciences

doi: 10.31210/spi2026.29.02.27
UDC 611.013.395:57.085.2:577.27
ORIGINAL ARTICLE

Scientific Progress & Innovations
ISSN: 2786-8842 (Print)
2786-8850 (Online)
29 (2)
2026

Comparative study of fresh and cryopreserved rat mesenchymal stem cells: cell viability, immunological gene expression, and cytokine production

G. K. Esmael

Article info

Correspondence Author
G. K. Esmael
E-mail:
ghassan.khudhair@qu.edu.iq

College of Veterinary Medicine, University of Al-Qadisiyah,
Al-Diwaniyah City,
Al-Qādisiyyah Governorate,
58002, Iraq

Citation: Esmael, G. K. (2026). Comparative study of fresh and cryopreserved rat mesenchymal stem cells: cell viability, immunological gene expression, and cytokine production. *Scientific Progress & Innovations*, 29(2), 193–204. doi: 10.31210/spi2026.29.02.27

Cryopreservation is fundamental for mesenchymal stem cell (MSC) banking, but the freeze–thaw cycle induces sub-cellular stress, potentially modifying the post-thaw genomic and paracrine identity of the cellular product. This study aimed to compare the biological, molecular, and functional stability of fresh and cryopreserved rat bone marrow MSCs (*Rattus norvegicus* BM-MSCs). Rat BM-MSCs were allocated into non-cryopreserved control cells (Fresh-MSCs) and cells frozen for 4 weeks in liquid nitrogen using 10 % DMSO (Cryo-MSCs). Cell survival was determined using the MTT assay. Immunoregulatory (*Il10, Tgfβ1, Ido1*) and apoptotic (*Bax, Casp3, Bcl2*) transcripts were evaluated via RT-qPCR. Paracrine protein concentrations of IL-10, TGF-β, TNF-α, IL-6, VEGF, and HGF were quantified via ELISA. Cryogenic processing significantly reduced post-thaw cell survival relative to fresh controls, though cellular viability safely remained high (87.32±2.91 % vs. 100.00±3.67 %; P<0.001). At the transcriptomic tier, Cryo-MSCs displayed a profound downregulation of all key immunomodulatory transcripts (P<0.05), with *Il10, Tgfβ1*, and *Ido1* levels dropping to 0.68±0.07, 0.77±0.06, and 0.61±0.06, respectively. This matched a 21.58 % and 21.87 % drop in secreted IL-10 and TGF-β protein concentrations (P≤0.05), running parallel to a 15 % to 20 % loss in the paracrine release of VEGF and HGF (P≤0.01). Conversely, cryogenic shock triggered an acute stress response that severely inverted the mitochondrial apoptosis ratio, inducing a significant 1.61-fold upsurge in pro-apoptotic *Bax* and a 1.49-fold increase in executioner *Casp3* transcripts, coupled with a 30.0 % reduction in survival-associated *Bcl2* mRNA (P≤0.05). This transcriptomic disruption reprogrammed the post-thaw secretome toward an inflammatory phenotype, characterized by a dramatic 2.12-fold and 1.59-fold escalation in secreted TNF-α and IL-6 protein levels, respectively (P≤0.05). Standard cryopreservation effectively preserves cell viability but causes a temporary operational impairment encompassing transcriptomic suppression of immunomodulatory networks, downregulatory trophic trends, and accelerated apoptotic signaling. These findings reveal compromised functional quality post-thaw, highlighting the clinical necessity for an optimized post-thaw acclimation incubation period prior to cell administration.

Keywords: mesenchymal stem cells (MSCs), cryopreservation, cell viability, immunomodulatory gene expression, cytokine secretion profile, paracrine trophic activity.

Порівняльне дослідження нативних і кріоконсервованих мезенхімальних стовбурових клітин щурів: життєздатність клітин, експресія імунологічних генів і продукція цитокінів

Г. Х. Есмаел

Факультет ветеринарної медицини, Університет Аль-Кадісія,
м. Ед-Дівання,
провінція Аль-Кадісія,
Ірак

Кріоконсервація є фундаментальним біопроцесом для банкінгу мезенхімальних стовбурових клітин (МСК), проте цикл заморожування-розморожування спричиняє субклітинний стрес, що потенційно модифікує посткріогенний геномний та секреторний профіль клітин. Це дослідження мало на меті порівняти біологічну, молекулярну та функціональну стабільність нативних і кріоконсервованих мезенхімальних стовбурових клітин кісткового мозку щурів (*Rattus norvegicus* BM-MSCs) після розморожування. МСК кісткового мозку щурів було розподілено на дві групи: некріоконсервовані контрольні клітини (Fresh-MSCs) та клітини, заморожені протягом 4 тижнів у рідкому азоті з використанням 10 % диметилсульфоксиду (Cryo-MSCs). Виживання клітин визначали за допомогою колориметричного аналізу з використанням 3-(4,5-диметилтіазол-2-іл)-2,5-дифенілтетразоліум броміду. Рівні експресії імунорегуляторних (*Il10*, *Tgfβ1*, *Ido1*) та апоптичних (*Bax*, *Casp3*, *Bcl2*) транскриптів оцінювали методом зворотної транскрипції з наступною кількісною ПЛР у реальному часі (ЗТ-кПЛР). Концентрації секретованих білків IL-10, TGF-β, TNF-α, IL-6, VEGF та HGF у супернатанті кількісно визначали за допомогою імуноферментного аналізу (ELISA). Процес кріоконсервації призвів до статистично значущого зниження виживання клітин після розморожування відносно нативного контролю, хоча життєздатність клітин залишалася на безпечно високому функціональному рівні (87,32±2,91 проти 100,00±3,67 %; P<0,001). На транскрипційному рівні у групі Cryo-MSCs виявлено глибоке пригнічення експресії всіх ключових імуномодулювальних транскриптів (P≤0,05), при цьому рівні *Il10*, *Tgfβ1* та *Ido1* знизилися до 0,68±0,07, 0,77±0,06 та 0,61±0,06 відповідно. Це узгоджувалося з падінням концентрацій секретованих протизапальних білків IL-10 та TGF-β на 21,58 та 21,87 % (P≤0,05), що відбувалося паралельно з втратою приблизно від 15 до 20 % паракринної секреції факторів VEGF та HGF (P≤0,01). Навпаки, кріогенний шок активував гостру стресову відповідь, яка суттєво порушила мітохондріальне співвідношення маркерів апоптозу, викликаючи значуще 1,61-кратне зростання проапоптичного транскрипту *Bax* та 1,49-кратне підвищення рівня ефекторної каспази *Casp3* на тлі 30,0 % зниження мРНК антиапоптичного гена *Bcl2* (P≤0,05). Виявлені зміни експресії генів призвели до функціонального перепрограмування секретому кріоконсервованих клітин після розморожування у бік запального фенотипу, що характеризувалося різким підвищенням рівнів секретованих білків TNF-α та IL-6 у 2,12 та 1,59 раза відповідно (P≤0,05). Стандартна кріоконсервація ефективно зберігає життєздатність клітин, проте викликає тимчасове погіршення їхнього функціонального стану, що охоплює транскрипційне пригнічення імуномодулювальних мереж, тенденцію до зниження продукції трофічних факторів та активацію проапоптичних сигнальних шляхів. Отримані результати свідчать про зниження функціональної якості МСК безпосередньо після розморожування, що підкреслює клінічну необхідність оптимізації періоду реакліматизації або інкубації клітинного продукту перед його введенням.

Ключові слова: мезенхімальні стовбурові клітини (МСК), кріоконсервація, життєздатність клітин, експресія імуномодулювальних генів, профіль секреції цитокінів, паракринна трофічна активність.

Бібліографічний опис для цитування: *Есмаел Г. Х.* Порівняльне дослідження нативних і кріоконсервованих мезенхімальних стовбурових клітин щурів: життєздатність клітин, експресія імунологічних генів і продукція цитокінів. *Scientific Progress & Innovations*. 2026. № 29 (2). С. 193–204.

Introduction

Mesenchymal stem cells (MSCs) represent a fundamental cornerstone of modern regenerative medicine and cellular biotechnology due to their extensive multilineage differentiation potential and potent immunomodulatory properties. Rather than relying solely on direct cellular replacement, these multipotent progenitors exert robust, long-range therapeutic effects that are primarily mediated by the active secretion of a dynamic secretome, which encompasses various pro-survival cytokines, angiogenic trophic factors, and anti-inflammatory macromolecules [1]. This complex paracrine signaling network allows MSCs to effectively modulate the host immune microenvironment, suppress excessive effector lymphocyte activation, and actively stimulate endogenous tissue repair pathways. Consequently, MSC-based cell therapies and cell-free products are being widely investigated globally for the clinical management of severe autoimmune diseases (such as systemic lupus erythematosus and rheumatoid arthritis), complex musculoskeletal disorders, chronic non-healing wounds, and progressive neurodegenerative conditions [2, 3].

Given their critical importance in clinical and research applications [4], establishing reliable long-term storage methods is essential. Cryopreservation protocols typically utilize ultra-low temperature storage in liquid nitrogen combined with dimethyl sulfoxide (DMSO) as a cryoprotectant to prevent intracellular ice crystal formation during the freezing and thawing cycles [5, 6]. However, the cryopreservation process itself poses significant challenges regarding its potential impact on the biological characteristics of MSCs. The physiological stresses of freezing and thawing often induce oxidative damage, osmotic shock, mitochondrial dysfunction, and cell membrane injury, which collectively compromise post-thaw cell viability [7].

Accumulating evidence indicates that cryopreserved MSCs frequently exhibit a reduced proliferative capacity, altered immunomodulatory activity, impaired paracrine secretion, and accelerated rates of apoptosis immediately after thawing compared with their fresh counterparts, thereby potentially diminishing their therapeutic efficacy [7]. The functional discrepancies between freshly isolated and cryopreserved-thawed MSCs – including variations in anti-inflammatory cytokine profiles and specific gene expression levels – remain a subject of intense investigation [2]. These biological alterations are largely dictated by specific cryopreservation protocols, storage duration, thawing rates, and the toxicity of cryoprotective agents. Therefore, comprehensive comparative studies are urgently required to systematically evaluate the molecular and functional consequences of cryopreservation [8].

The aim of the study

The present study aimed to comprehensively evaluate and compare the functional stability of freshly isolated and cryopreserved-thawed rat bone marrow mesenchymal stem cells (*Rattus norvegicus* BM-MSCs). Specifically, the current work was designed to investigate the immediate impact of the freeze–thaw cycle on essential post-thaw biological activities by systematically assessing cellular viability, apoptosis-associated genomic shifts, immunomodulatory gene expression patterns, and the quantitative paracrine secretion profiles of key cytokines and growth factors.

Materials and methods

Study design

The present study was conducted *in vitro* to systematically evaluate and compare the biological, molecular, and functional characteristics of fresh and cryopreserved rat bone marrow-derived mesenchymal stem cells (BM-MSCs). The experimental parameters focused on assessing cell viability, apoptosis-related gene expression profiles, immunomodulatory gene transcription, and the paracrine secretion of cytokines and growth factors.

MSCs culture and expansion

Rat BM-MSCs were obtained from Cell Biologics Company (USA). The cells were maintained and expanded under standardized culture conditions in Dulbecco's Modified Eagle Medium (DMEM) supplemented with 10 % fetal bovine serum (FBS), 1 % penicillin-streptomycin, and L-glutamine. Cultured cells were incubated in a humidified atmosphere at 37°C with 5 % CO_2. The culture medium was routinely replenished every 48 hours. To ensure physiological and phenotypic stability, cells at low passages (passages 3–5) were utilized for all downstream experimental procedures.

Experimental groups

To investigate the precise effects of the freeze–thaw cycle, the expanded BM-MSCs were divided into two distinct experimental groups:

- Group 1 (Fresh-MSCs): Cultured cells maintained continuously under standard incubation conditions without undergoing cryopreservation.
- Group 2 (Cryo-MSCs): Cells subjected to ultra-low temperature cryopreservation and subsequently thawed for analysis.

To ensure statistical reliability, all independent experimental runs were performed in triplicate.

Cryopreservation and thawing protocols

For the cryopreservation procedure, BM-MSCs were harvested utilizing 0.25 % trypsin-EDTA, washed with phosphate-buffered saline (PBS), and resuspended at a definitive density of 1×10^6 cells/mL. The cryopreservation medium consisted of 90 % FBS and 10 % dimethyl sulfoxide (DMSO) as a cryoprotective agent [5, 6]. Cell suspensions were transferred to cryovials and initially cooled at a controlled rate of −1°C/minute using a specialized freezing container before storage at −80°C. After 24 hours, the cryovials were transferred to liquid nitrogen (−196°C) for a long-term storage period of 4 weeks.

For the thawing procedure, the cryovials were rapidly removed from liquid nitrogen and immediately submerged in a water bath at 37°C with gentle agitation. To mitigate the cytotoxic effects of DMSO upon thawing,

the cell suspension was immediately diluted with a 10-fold volume of fresh pre-warmed culture medium. The cells were then centrifuged at 300 × g for 5 minutes, and the resulting pellet was resuspended in fresh complete culture medium. The thawed BM-MSCs were cultured overnight to allow cellular stabilization prior to subsequent biological and molecular analyses.

Cell viability assay

Cell viability was quantitatively evaluated using the standard 3-(4,5-dimethylthiazol-2-yl)-2,5-diphenyltetrazolium bromide (MTT) assay. Briefly, BM-MSCs from both experimental groups were seeded into 96-well culture plates at a density of 5×10^3 cells per well and maintained in a humidified incubator. Following the overnight stabilization period, the MTT reagent (5 mg/mL) was added to each well, and the plates were incubated at 37°C for an additional 4 hours. After incubation, the supernatant was carefully removed, and the resulting converted intracellular formazan crystals were completely dissolved in DMSO. The absorbance of each well was measured at a wavelength of 570 nm using a microplate reader. Post-thaw cell viability was calculated and expressed as a percentage relative to the control group (Fresh-MSCs), which was defined as 100 % viable.

Primer design and synthesis

Oligonucleotide primers for the target rat genes were strategically designed using the online Primer3Plus software, based on reference mRNA sequences retrieved from the National Center for Biotechnology Information (NCBI) GenBank database. All primers were commercially synthesized and purified. The specific forward (F) and reverse (R) primer sequences, along with their expected amplicon sizes and NCBI reference sequence numbers, are comprehensively detailed in ***Table 1***.

Table 1

Oligonucleotide primer sequences used for quantitative real-time PCR analysis

Target gene	Forward primer sequence (5′–3′)	Reverse primer sequence (5′–3′)	Product size (bp)	NCBI RefSeq accession No.
Il10	CCTGCTCTTACTGGCTGGAG	TGTCCAGCTGGTCCTTCTTT	188	NM_012854.2
Tgfβ1	CTGGAGGCTGAGGCAATAAG	AGAAGGCAGAGGTGAGTGGA	225	NC_086019.1
Ido1	CGTGGATCCAGACACCTTTT	GGCTGGAGGCATGTACTCTC	247	NM_023973.2
Bax	TGCAGCCTTTGTCCTCTTTT	GGGACGGCTCACACTGTAAT	159	NC_086019.1
Casp3	GATTCAACGCTGAGCAAACA	CTCCCAAGGGCCTAGATTTC	227	NC_086034.1
Bcl2	GCCAGTGTTGGCTTTACCAT	CTACTGCCGAAAATGGTGGT	150	NC_086031.1

RNA extraction and quantitative real-time PCR (RT-qPCR)

Total RNA extraction from both Fresh-MSCs and Cryo-MSCs was performed utilizing a commercially available total RNA isolation kit according to the manufacturer's instructions. The concentration and purity of the isolated RNA were spectrophotometrically assessed. Total RNA was subsequently reverse-transcribed into complementary DNA (cDNA) using a high-capacity cDNA reverse transcription kit. Quantitative real-time PCR (qPCR) amplifications were performed using a SYBR Green PCR Master Mix on a real-time PCR detection system. The relative expression levels of the target genes (*Il10*, *Tgfβ1*, *Ido1*, *Bax*, *Casp3*, and *Bcl2*) were measured and normalized to the expression of Glyceraldehyde 3-phosphate dehydrogenase (*Gapdh*), which served as the internal housekeeping reference gene. The relative fold changes in gene expression were calculated using the comparative $2^{-\Delta\Delta Ct}$ method (the Livak method) [10].

Cytokine and growth factor quantification via ELISA

To evaluate the paracrine secretory profile, the cell culture supernatants were harvested 24 hours post-seeding. The collected media were centrifuged to remove residual cellular debris and stored in aliquots at −80°C until further analysis. Commercially available enzyme-linked immunosorbent assay (ELISA) kits were utilized to quantitatively determine the protein concentrations of interleukin-10 (IL-10), transforming growth factor-beta (TGF-β), tumor necrosis factor-alpha (TNF-α), interleukin-6 (IL-6), vascular endothelial growth factor (VEGF), and hepatocyte growth factor (HGF). The absorbance of each sample was measured using a microplate reader at the recommended wavelength, and final protein levels were calculated based on the respective standard curves generated according to the manufacturer's technical directions.

Statistical Analysis

All experimental procedures were performed independently in triplicate, and the resulting data are expressed as the mean ± standard deviation (SD). Statistical analyses were executed using GraphPad Prism software (version 10.0; GraphPad Software, USA). Discrepancies and differences between the two experimental groups (Fresh-MSCs vs. Cryo-MSCs) were systematically evaluated utilizing the independent-samples Student's *t*-test. Statistical significance was predefined and established at a threshold of $P<0.05$.

Results and discussion

Cell viability analysis

To evaluate the immediate impact of the freeze – thaw cycle on cellular survival, post-thaw cell viability was quantitatively assessed via the colorimetric MTT assay and systematically compared with that of the non-cryopreserved control population, as detailed in ***Table 2***. This enzymatic evaluation was fundamentally based on the capacity of mitochondrial succinate dehydrogenase enzymes within metabolically active, surviving BM-MSCs to reduce the yellow tetrazolium salt into insoluble purple formazan crystals. The quantitative optical density profiles, which directly correlate with the total pool of structurally intact and viable cells surviving the

cryopreservation and thawing protocols, were precisely captured to map the exact percentage of cellular recovery.

Table 2

Quantitative evaluation of post-thaw cell viability in Fresh-MSCs and Cryo-MSCs via MTT assay, Mean±SD

Experimental group	Cell viability, %	Statistical significance
Fresh-MSCs	100.00±3.67	a
Cryo-MSCs	87.32±2.91	b
P-value	< 0.001	*

Note: Different superscript letters (a, b) within the same column indicate a statistically significant difference between the experimental groups (P≤0.01). Asterisk (*) denotes high statistical significance (P<0.001).

The quantitative analysis demonstrated that the cryopreservation and thawing processes induced a highly significant reduction in cellular survival capacity compared with the non-cryopreserved control population (P<0.001). Specifically, cell viability was significantly decreased in the Cryo-MSCs group relative to the baseline Fresh-MSCs group (P<0.001, ***Table 2***). These experimental data confirm that cryogenic stress triggers a statistically verified wave of cell mortality; however, the absolute majority of the rat bone marrow mesenchymal stem cells successfully survived the utilized storage and thawing protocol, maintaining robust baseline viability.

Expression of immunomodulatory genes

To evaluate the molecular alterations underlying the immunomodulatory potential of rat BM-MSCs following cryogenic stress, the relative mRNA transcription levels of interleukin-10 (*Il10*), transforming growth factor-beta 1 (*Tgfβ1*), and indoleamine 2,3-dioxygenase 1 (*Ido1*) were quantitatively analyzed via RT-qPCR, with the comparative datasets detailed in ***Table 3***.

Table 3

Relative mRNA expression levels of immunomodulatory genes (*Il10*, *Tgfβ1*, and *Ido1*) in Fresh-MSCs and Cryo-MSCs, Mean±SD

Target gene	Fresh-MSCs	Cryo-MSCs	Statistical significance
Il10	1.00±0.09 (a)	0.68±0.07 (b)	*
Tgfβ1	1.00±0.10 (a)	0.77±0.06 (b)	*
Ido1	1.00±0.08 (a)	0.61±0.06 (b)	*

Note: Data are expressed as relative fold changes ($2^{-\Delta\Delta Ct}$) normalized to the baseline of the Fresh-MSCs group (defined as 1.00). Different letters (a, b) within the same row indicate a statistically significant difference between the experimental groups (P≤0.05). The asterisk (*) denotes a statistically significant downregulation.

The real-time PCR analysis demonstrated a statistically significant downregulation in the transcriptional activity of all investigated immunomodulatory markers within the cryopreserved cell population post-thaw (P≤0.05). Specifically, the relative mRNA expression levels of *Il10*, *Tgfβ1*, and *Ido1* were significantly decreased in the Cryo-MSCs group compared with the non-cryopreserved control population (P≤0.05, ***Table 3***). These molecular findings confirm that while cells remain structurally intact and viable, cryogenic processing triggers a significant operational suppression of key anti-inflammatory and immunosuppressive transcripts immediately after the thawing procedure.

Real-time PCR kinetic analysis for Il10 gene

The transcriptional amplification kinetics and threshold cycle values for the targeted anti-inflammatory gene were systematically monitored in real time, with the representative fluorescence accumulation curves for both experimental groups depicted in ***Figure 1***.

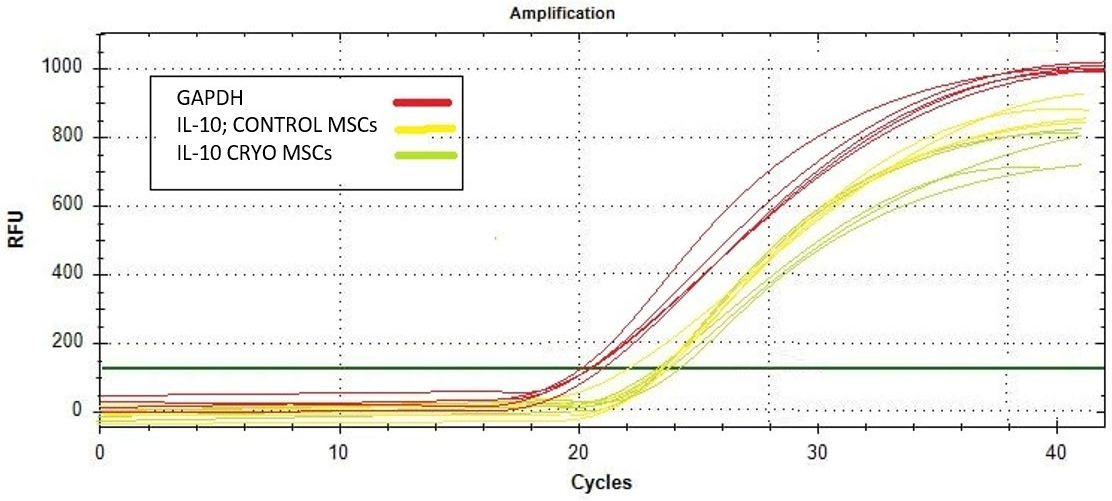

Fig. 1. Real-time PCR amplification curves for the *Il10* gene in Fresh-MSCs and Cryo-MSCs groups

The kinetic magnification profiles illustrate the real-time exponential accumulation of fluorescence signal for the target *Il10* transcript relative to the internal reference gene (*Gapdh*). The threshold cycle (C_t) values, represented by the intersection points of the amplification curves with the fixed horizontal baseline (green line), show a clear rightward shift for the cryopreserved cell population (Cryo-MSCs) compared with the non-cryopreserved control group (Fresh-MSCs). This graphical shift in amplification curves directly reflects a higher C_t value, visually demonstrating a substantial reduction in the baseline template copy number of *Il10* mRNA in mesenchymal stem cells immediately following the freeze – thaw and cryopreservation procedures.

Real-time PCR kinetic analysis for Tgfβ1 gene

The transcriptional amplification kinetics and corresponding threshold cycle values for transforming growth factor-beta 1 were continuously recorded during the exponential phase of the reaction, with the comparative fluorescence accumulation curves illustrated in ***Figure 2***.

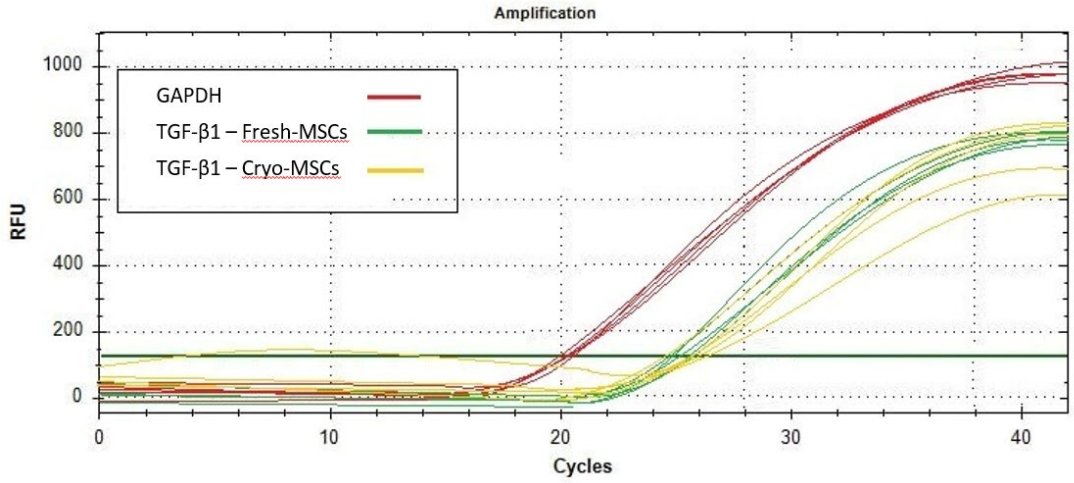

Fig. 2. Real-time PCR amplification curves for the *Tgfβ1* gene in Fresh-MSCs and Cryo-MSCs groups

The real-time amplification profiles track the logarithmic accumulation of the fluorescent signal for the target *Tgfβ1* gene and the internal control (*Gapdh*). The point of intersection where the amplification signal crosses the baseline threshold (indicated by the horizontal green line) demonstrates a noticeable rightward delay for the cryopreserved cell sample (Cryo-MSCs) relative to the fresh sample (Fresh-MSCs). This spatial shift on the horizontal axis indicates an increased threshold cycle (C_t) value for the Cryo-MSCs, visually substantiating a marked decrease in the initial amount of target *Tgfβ1* mRNA transcripts in the cells after undergoing the cryopreservation and thawing protocol.

Real-time PCR kinetic analysis for Ido1 gene

The transcriptional amplification kinetics and corresponding threshold cycle values for indoleamine 2,3-dioxygenase 1 were continuously recorded during the exponential phase of the reaction, with the comparative fluorescence accumulation curves illustrated in ***Figure 3***.

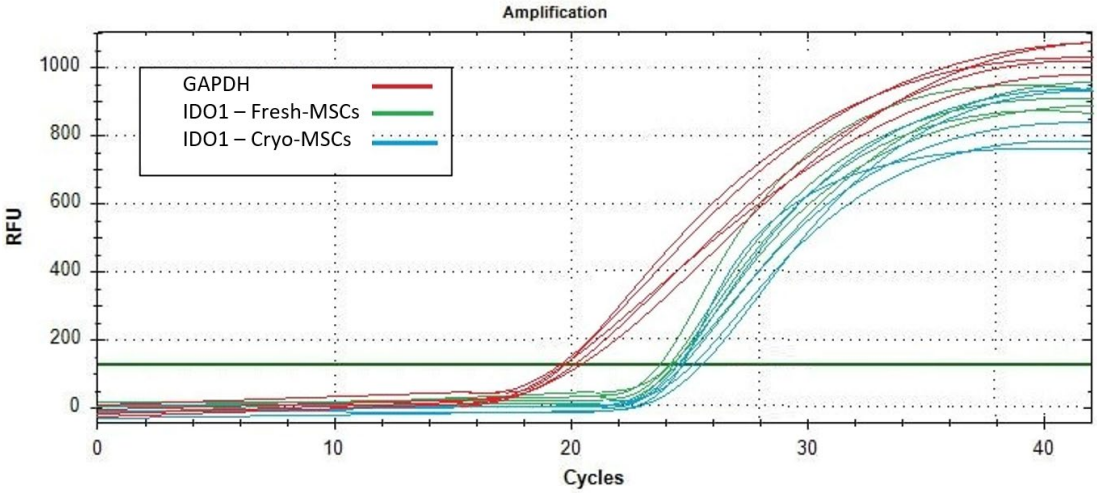

Fig. 3. Real-time PCR amplification curves for the *Ido1* gene in Fresh-MSCs and Cryo-MSCs groups

The real-time amplification profiles track the logarithmic accumulation of the fluorescent signal for the target *Ido1* gene and the internal control (*Gapdh*). The point of intersection where the amplification signal crosses the baseline threshold (indicated by the horizontal green line) demonstrates a noticeable rightward delay for the cryopreserved cell sample (Cryo-MSCs) relative to the fresh sample (Fresh-MSCs). This spatial shift on the horizontal axis indicates an increased threshold cycle (C_t) value for the Cryo-MSCs, visually substantiating a marked decrease in the initial amount of target *Ido1* mRNA transcripts in the cells after undergoing the cryopreservation and thawing protocol.

Expression of apoptosis-related genes

To systematically evaluate the molecular pathways triggering programmed cell death following cryogenic stress, the relative mRNA transcription levels of the pro-apoptotic markers (*Bax*, *Casp3*) and the anti-apoptotic regulator (*Bcl2*) were quantitatively analyzed via RT-qPCR, with the comparative datasets detailed in ***Table 4***.

Table 4

Relative mRNA expression levels of apoptosis-related genes (*Bax*, *Casp3*, and *Bcl2*) in Fresh-MSCs and Cryo-MSCs, Mean±SD

Target gene	Fresh-MSCs	Cryo-MSCs	Statistical significance
Bax	1.00±0.03 (b)	1.61±0.11 (a)	*
Casp3	1.00±0.08 (b)	1.49±0.10 (a)	*
Bcl2	1.00±0.02 (a)	0.70±0.09 (b)	*

Note: Data are expressed as relative fold changes ($2^{-\Delta\Delta Ct}$) normalized to the baseline of the Fresh-MSCs group (defined as 1.00). Different letters (a, b) within the same row indicate a statistically significant difference between the experimental groups (P≤0.05). The asterisk (*) denotes a statistically significant alteration.

The real-time PCR analysis demonstrated a highly significant molecular shift toward the transcriptional activation of programmed cell death pathways within the cryopreserved cell population post-thaw (P≤0.05). Specifically, the relative mRNA expression levels of the key pro-apoptotic initiator *Bax* and the main executioner caspase *Casp3* were significantly increased in the Cryo-MSCs group compared with the baseline fresh control population (P≤0.05, ***Table 4***). Concurrently, the transcriptional activity of the vital survival-associated gene *Bcl2* was significantly decreased in the stored cells (P≤0.05). This simultaneous disruption of the pro- and anti-apoptotic genomic balance confirms that cryogenic processing directly triggers an activation of downstream caspase-dependent apoptotic mechanisms immediately after thawing.

Real-time PCR kinetic analysis for Bax gene

The transcriptional amplification kinetics and threshold cycle values for the targeted pro-apoptotic gene were monitored in real time during the reaction, with the representative fluorescence accumulation curves for both experimental groups illustrated in ***Figure 4***.

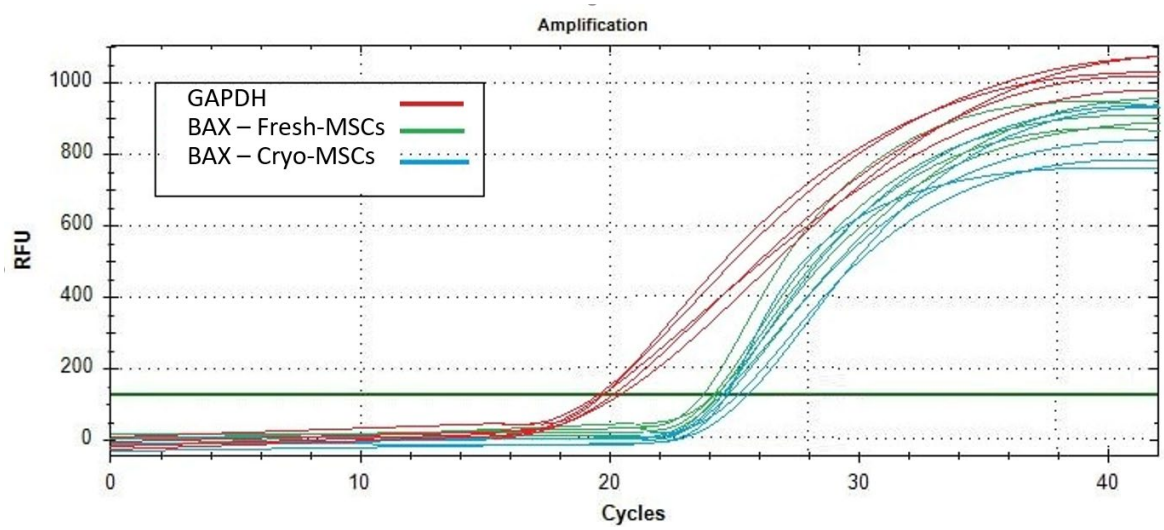

Fig. 4. Real-time PCR amplification curves for the pro-apoptotic *Bax* gene in Fresh-MSCs and Cryo-MSCs groups

The real-time amplification profiles track the logarithmic accumulation of the fluorescent signal for the target pro-apoptotic *Bax* gene relative to the internal housekeeping control (*Gapdh*). The threshold cycle (C_t) values, represented by the points where the fluorescence amplification signals cross the fixed horizontal baseline (green line), demonstrate a distinct leftward shift for the cryopreserved cell population (Cryo-MSCs) compared with the non-cryopreserved fresh control group (Fresh-MSCs). This spatial shift on the horizontal axis indicates a significantly lower C_t value for the Cryo-MSCs, visually confirming an immediate post-thaw upsurge in template copy numbers and demonstrating that cryogenic processing triggers an immediate transcriptional activation of cell-death pathways.

Real-time PCR kinetic analysis for Casp3 gene

The transcriptional amplification kinetics and threshold cycle values for the major executioner caspase gene were monitored in real time during the reaction, with the representative fluorescence accumulation curves for both experimental groups illustrated in ***Figure 5***.

The real-time amplification profiles track the logarithmic accumulation of the fluorescent signal for the target apoptotic gene *Casp3* relative to the internal housekeeping control (*Gapdh*). The threshold cycle (C_t) values, represented by the points where the fluorescence amplification signals cross the fixed horizontal baseline (green line), demonstrate a distinct leftward shift for the cryopreserved cell population (Cryo-MSCs) compared with the non-cryopreserved fresh control group (Fresh-MSCs). This spatial shift on the horizontal axis indicates a significantly lower C_t value for the Cryo-MSCs, visually confirming an immediate post-thaw upsurge in template copy numbers and demonstrating that cryogenic processing triggers an immediate transcriptional activation of downstream caspase-dependent apoptotic pathways.

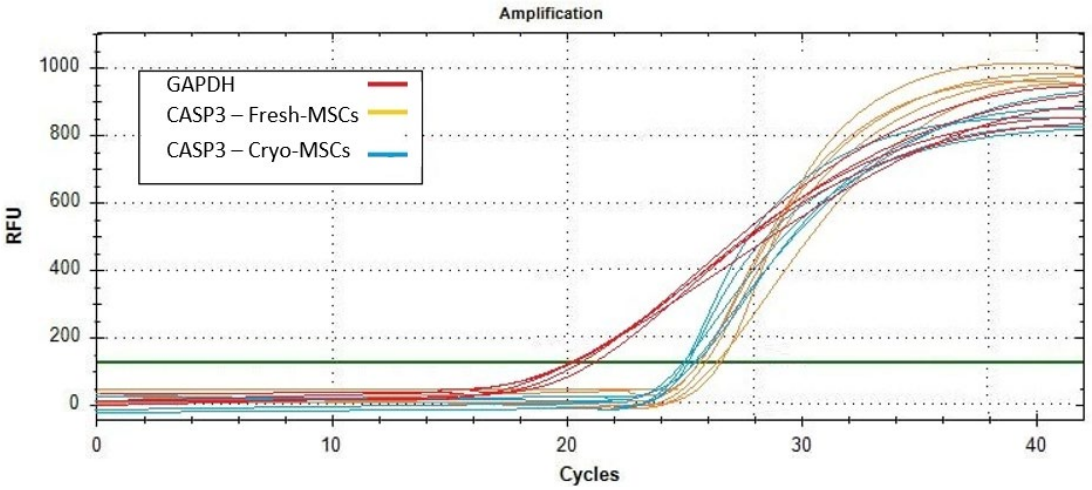

Fig. 5. Real-time PCR amplification curves for the executioner *Casp3* gene in Fresh-MSCs and Cryo-MSCs groups

Real-time PCR kinetic analysis for Bcl2 gene

The transcriptional amplification kinetics and corresponding threshold cycle values for the protective anti-apoptotic regulator gene were monitored in real time during the reaction, with the representative fluorescence accumulation curves for both experimental groups illustrated in ***Figure 6***.

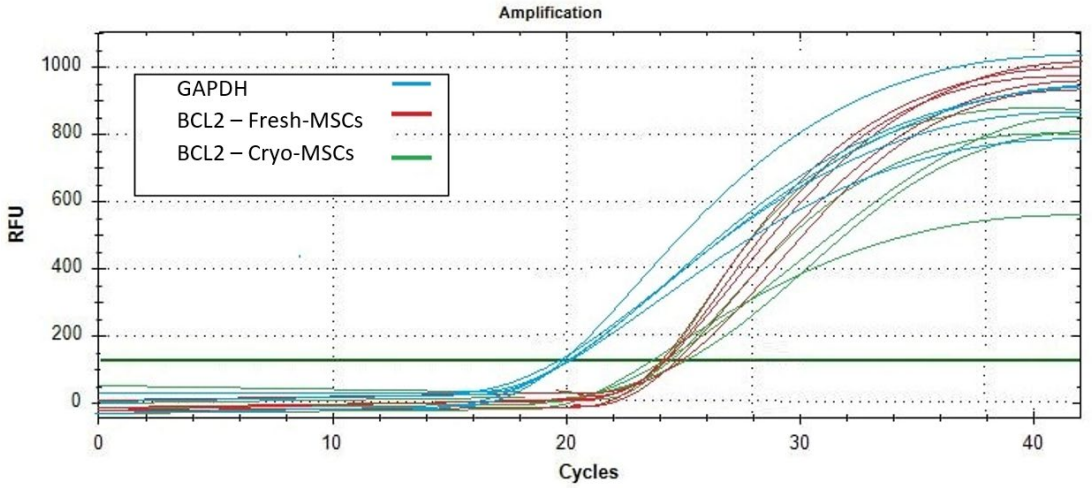

Fig. 6. Real-time PCR amplification curves for the anti-apoptotic *Bcl2* gene in Fresh-MSCs and Cryo-MSCs groups

The real-time amplification profiles track the logarithmic accumulation of the fluorescent signal for the target survival-associated gene *Bcl2* relative to the internal housekeeping control (*Gapdh*). The threshold cycle (C_t) values, represented by the points where the fluorescence amplification signals cross the fixed horizontal baseline (green line), demonstrate a distinct rightward delay for the cryopreserved cell population (Cryo-MSCs) compared with the non-cryopreserved fresh control group (Fresh-MSCs). This spatial shift on the horizontal axis indicates a significantly higher C_t value for the Cryo-MSCs, visually substantiating a marked downregulation of protective anti-apoptotic transcripts following cryogenic processing and confirming that the freeze – thaw stress compromises the cellular survival machinery.

Cytokine secretion profile

To evaluate the impact of cryogenic stress on the paracrine immunomodulatory activity of rat BM-MSCs, the concentrations of key anti-inflammatory (IL-10, TGF-β) and pro-inflammatory (TNF-α, IL-6) cytokines secreted into the culture supernatant were quantitatively measured via ELISA, with the comparative data detailed in ***Table 5***.

Table 5

Concentrations of secreted cytokines (IL-10, TGF-β, TNF-α, and IL-6) in Fresh-MSCs and Cryo-MSCs supernatants, Mean±SD

Cytokine	Fresh-MSCs, pg/mL	Cryo-MSCs, pg/mL	Statistical significance
IL-10	197.40±8.80 (a)	154.80±7.70 (b)	*
TGF-β	439.80±17.40 (a)	343.60±13.30 (b)	*
TNF-α	13.60±2.40 (b)	28.90±3.60 (a)	*
IL-6	24.40±2.80 (b)	38.70±2.10 (a)	*

Note: Different letters (a, b) within the same row indicate a statistically significant difference between the experimental groups ($P \leq 0.05$). The asterisk (*) denotes a high level of statistical significance ($P < 0.05$).

The quantitative protein analysis revealed a definitive, statistically significant shift in the paracrine secretory profile of stored cells post-thaw, characterized by a

suppression of protective factors and a concurrent upregulation of inflammatory mediators (P≤0.05, ***Table 5***). Specifically, the secretion of vital anti-inflammatory cytokines was significantly decreased in the Cryo-MSCs group (P≤0.05), with IL-10 and TGF-β protein concentrations experiencing a 21.58 % and 21.87 % reduction, respectively, relative to the baseline fresh controls.

Conversely, the release of classical pro-inflammatory cytokines into the supernatant was significantly increased following the freeze – thaw process (P≤0.05). Quantitatively, secreted TNF-α levels experienced a dramatic 2.12-fold increase (P≤0.05), effectively more than doubling the baseline level, while IL-6 secretion rose prominently by 1.59-fold (P≤0.05) in the cryopreserved population compared with the non-cryopreserved control cells. These findings substantiate at the protein level that while cryogenic stabilization maintains cell survival, it triggers a significant functional reprogramming of the MSC secretome, downregulating anti-inflammatory defenses while expanding the release of central inflammatory triggers in multiple times immediately after thawing.

Growth factor secretion profile

To evaluate the impact of the freeze–thaw cycle on the trophic and regenerative potential of rat BM-MSCs, the protein concentrations of vascular endothelial growth factor (VEGF) and hepatocyte growth factor (HGF) released into the culture supernatant were quantified via ELISA, with the comparative datasets summarized in ***Table 6***.

Table 6

Concentrations of secreted trophic factors (VEGF and HGF) in Fresh-MSCs and Cryo-MSCs supernatants, Mean±SD

Growth factor	Fresh-MSCs, pg/mL	Cryo-MSCs, pg/mL	Statistical significance
VEGF	739.90±24.40 (a)	590.20±24.80 (b)	*
HGF	911.60±39.90 (a)	766.90±29.20 (b)	*

Note: Different letters (a, b) within the same row indicate a statistically significant difference between the experimental groups (P≤0.01). The asterisk (*) denotes a high level of statistical significance (P≤0.01).

The enzyme-linked immunosorbent assay revealed a highly significant reduction in the secretory output of trophic and angiogenic factors in mesenchymal stem cells subjected to cryopreservation (P≤0.01, ***Table 6***). Specifically, following the freeze–thaw cycle, the paracrine release of vascular endothelial growth factor (VEGF) was significantly decreased by 20.23 % in the Cryo-MSCs group compared with the robust baseline production of the fresh controls (P≤0.01). Concurrently, the protein levels of the vital regenerative factor hepatocyte growth factor (HGF) were also significantly decreased by 15.87 % post-thaw (P≤0.01). These results mathematically substantiate at the protein level that cryogenic stresses modify the regenerative identity of the MSC secretome, causing an immediate, measurable impairment in their paracrine therapeutic capacity.

The evaluation of cellular viability post-thawing represents a fundamental metric for assessing the quality and structural preservation of mesenchymal stem cells following cryogenic storage. In the present study, the cryopreservation and thawing cycle induced a statistically significant downregulation in rat BM-MSC survival capacity compared with the freshly isolated control population. Nevertheless, despite the measurable reduction in active cellular numbers, the post-thaw viability remained robust, firmly demonstrating that the critical majority of the BM-MSC pool successfully survived the physiological stresses of ultra-low temperature stabilization, which strongly aligns with earlier methodological findings [9].

The observed decline in post-thaw survival is consistent with documented consensus indicating that cryogenic processing invariably imposes mechanical and osmotic strains on cell membranes. For instance, a precise quantitative assessment of human bone marrow-derived MSCs revealed a comparable immediate drop in post-thaw viability relative to fresh cells [10]. Furthermore, variations in post-thaw survival have been widely linked to specific preservation parameters; prior investigations using diverse cryoprotective formulations reported a broad viability range of 63–81 % depending on the specific agent utilized [11]. Although another study documented a slightly higher post-thaw recovery rate of 94.3 %, the overarching trend of a significant cryopreservation-induced viability decrease remains identical, confirming that the viability rate captured in our experiment tightly falls within previously validated acceptable parameters [12].

It is important to highlight that cryogenic injury does not uniformly result in permanent or severe functional impairment. Several investigators have successfully achieved post-thaw survival rates exceeding 90%, noting that cryopreserved MSC fractions consistently retain the key biological and phenotypic traits characteristic of the fresh parental cell line [13]. This functional resilience is further supported by multi-conditional storage evaluations where cryopreserved cells demonstrated post-thaw viability above 95%, exhibiting rapid metabolic recovery and displaying no significant deviations in differentiation capacity or morphological characteristics compared with non-cryopreserved controls [7].

Prior evidence indicates that cryopreserved MSCs can preserve key phenotypic hallmarks despite exhibiting partial, transient impairments in their multi-lineage differentiation capacity. Consequently, the biological impact of cryogenic stabilization cannot be adequately described by survival rates alone, as a baseline reduction in viability does not necessarily imply that the surviving cellular fraction has lost its overall therapeutic and functional potency [14]. The numerical discrepancies reported across literature primarily reflect variations in experimental conditions, rather than fundamental contradictions in cellular biology. Cryopreservation inherently exposes cells to successive thermodynamic stresses, including acute osmotic shifts, cold shock, and intracellular or extracellular ice crystal formation [15]. The magnitude of this cellular damage is heavily dictated by freezing kinetics, cryoprotectant formulations, and the

baseline cellular physiological state [16]. Therefore, the post-thaw survival rate captured in our study must be interpreted strictly within the context of the utilized protocol parameters. Furthermore, the precise timing of post-thaw analysis plays a critical role, as cryopreservation-associated injury and apoptosis pathways often undergo a progressive escalation during the early post-thawing incubation period [10].

At the transcriptomic level, our study demonstrated that cryogenic processing induces a significant operational suppression of key immunoregulatory genes, including interleukin-10 (*Il10*), transforming growth factor-beta 1 (*Tgfβ1*), and indoleamine 2,3-dioxygenase 1 (*Ido1*). These specific molecular markers serve as central components of the MSC-mediated immunosuppressive machinery, where IL-10 and TGF-β1 drive the resolution of excessive inflammatory immune responses, and IDO1 acts as a pivotal metabolic mediator capable of directly modulating lymphocyte activation and proliferation [17]. Documented consensus establishes that MSC-driven immunoregulation relies on the coordinated expression of these inhibitory networks; however, their relative activation and functional contribution are dynamic and remain highly sensitive to the surrounding cellular microenvironment and the nature of specific inflammatory licensing stimuli [18].

The transcriptional downregulation observed in our experiment is consistent with reports indicating that cryopreservation induces a transient functional alteration in the immunomodulatory phenotype of MSCs. Specifically, thawed cells frequently exhibit an impaired responsiveness to inflammatory licensing signals, such as interferon-gamma (IFN-γ), leading to a severely reduced capacity to upregulate *Ido1* expression and suppress T-cell proliferation immediately post-thaw [19]. Importantly, these compromised properties are typically restored after a short period of post-thaw culture (often within 24 hours), demonstrating that the immediate cryogenic shock reflects an altered metabolic state rather than an irreversible or permanent loss of the intrinsic immunomodulatory potential of MSCs [20].

The parallel reduction of *Il10* and *Tgfβ1* transcripts further underscores this temporary operational depression within the broader context of MSC-mediated immune regulation. These molecules do not function as isolated genetic markers; rather, they form an interconnected immunomodulatory network that drives the suppression of T-lymphocyte activation. Prior co-culture investigations have demonstrated a direct correlation between elevated *Il10* and *Tgfβ* transcript numbers and the potency of MSC-mediated inhibitory effects on effector cell expansion [21]. Consequently, the significant baseline downregulation of these key immunoregulatory axes captured in our study indicates that cryogenic processing temporarily minimizes the immediate post-thaw anti-inflammatory paracrine capacity of the cells prior to their full metabolic stabilization.

Although literature presents some apparent discrepancies regarding the threshold of functional impairment induced by freezing – with certain trials demonstrating that high post-thaw viability correlates with a retained capacity to suppress activated T-cells [22] – several compounding factors must be considered.

Crucially, the significant transcriptomic downregulation identified in our study – where relative mRNA levels of *Il10*, *Tgfβ1*, and *Ido1* dropped to 0.68±0.07, 0.77±0.06, and 0.61±0.06, respectively – represents only a single regulatory tier of biological activity [12]. This operational depression captured under unstimulated culture conditions reflects a transient post-thaw shock rather than an irreversible loss of potency, as enzyme systems like IDO1 remain highly inducible by environmental danger signals like IFN-γ [20].

Furthermore, while prior works suggested that molecular alterations require extensive subsequent verification at the translational level [8], our transcriptomic findings are directly corroborated by our own protein-level data. The fact that actual IL-10 and TGF-β protein secretion decreased by 21.58 % and 21.87 % in the Cryo-MSCs supernatant mathematically validates that the transcription-level suppression effectively translates into a measurable, immediate impairment of the anti-inflammatory paracrine profile.

This cryogenic suppression of the immunoregulatory machinery is tightly linked to the systematic activation of programmed cell death pathways. Following the freeze – thaw cycle, our data revealed a highly significant shift in the mitochondrial survival ratio, characterized by a 1.61-fold increase in pro-apoptotic *Bax* expression and a 1.49-fold upsurge in executioner *Casp3* transcripts, coupled with a 30.0 % reduction in protective *Bcl2* mRNA.

This precise genomic imbalance provides a robust molecular foundation for the immediate post-thaw cryogenic shock, aligning with baseline stress models where a 1.5-fold to 2-fold acceleration of caspase-dependent apoptotic entry was documented within the early 24-hour post-thaw incubation period [23, 24]. The parallel activation of these cell-death cascades confirms that despite maintaining an acceptable morphological cell survival, cryogenic processing forces a significant fraction of the surviving cellular population to undergo a transient apoptotic stress immediately after the thawing procedure.

The synchronized behavior of *Bax* and *Bcl2* transcripts documented in our experiment further substantiates the involvement of mitochondrial-driven cell death pathways. The intracellular ratio between pro-apoptotic and anti-apoptotic members of the Bcl-2 family serves as a master rheostat governing mitochondrial outer membrane permeabilization and subsequent cell survival. In the current study, the simultaneous induction of *Bax* and a 30.0 % reduction in *Bcl2* transcripts shifts the intracellular equilibrium toward an environment highly permissive to programmed cell death. This molecular pattern strongly mirrors experimental models of cryoinjury, where the activation of Bcl-2-regulated mitochondrial cascades was heavily implicated in freeze–thaw damage, whereas forced upregulation of protective Bcl-2 proteins consistently shielded cells from cryogenic stress [24].

Crucially, the ultimate impact of cryopreservation on cellular apoptosis must be interpreted as a dynamic, rather than uniform or irreversible, phenomenon. Kinetic

tracking during the early post-thaw period demonstrates that apoptotic signaling typically experiences an acute spike during the initial hours after thawing, followed by a gradual stabilization as the surviving population recovers metabolic equilibrium. Prior evaluations in human MSCs confirmed that cryogenic injury triggers an immediate upsurge in apoptotic cascades within the first 4 hours post-thaw; however, by the 24-hour mark, viability parameters experience a partial recovery alongside a notable decline in active cell death markers [10].

Given that our methodology utilized an overnight incubation period prior to analysis, the 1.61-fold and 1.49-fold elevation in *Bax* and *Casp3* transcripts captured in our study likely reflects the active molecular footprint of this early post-thaw recovery phase, rather than a definitive trajectory toward total population mortality. The ultimate magnitude of this cryoinjury is highly variable, dictated by specific freezing kinetics, cryoprotectant toxicity, cell density, and the composition of the post-thaw culture medium [8]. Because MSCs represent inherently heterogeneous cellular populations, the surviving cellular fraction frequently retains substantial functional and immunomodulatory potency even when elevated apoptotic gene expression remains temporarily detectable at the molecular level [25].

The simultaneous transcriptional upregulation of *Bax* and *Casp3* alongside the concomitant downregulation of *Bcl2* strongly demonstrates that the freeze – thaw process temporarily destabilizes the molecular equilibrium governing cell survival. The absolute magnitude and chronological persistence of this intracellular stress response are highly dependent on specific cryopreservation protocol parameters and the precise post-thaw evaluation window. Consequently, this transient genomic shift should be interpreted as an immediate, adaptive molecular response to cryogenic stress rather than as definitive evidence of irreversible structural loss or total population mortality [23].

At the translational level, this cryogenic stress triggers a distinct, statistically verified functional reprogramming of the mesenchymal stem cell secretome. Our quantitative protein analyses demonstrated a significant paracrine shift away from the highly active immunoregulatory and trophic profile characteristic of fresh cells toward an inflammatory phenotype. Specifically, the fact that the secretion of vital anti-inflammatory cytokines IL-10 and TGF-β dropped by 21.58 % and 21.87 %, respectively, post-thaw carries substantial clinical relevance, given that these specific mediators drive the suppression of excessive inflammatory signaling and govern peripheral immune-cell activation.

A significant reduction in the baseline release of both factors mathematically validates that cryogenic processing temporarily compromises the immediate capacity of BM-MSCs to establish a protective, anti-inflammatory paracrine microenvironment. However, prior functional recovery models indicate that this altered post-thaw phenotype is transient; the documented restoration of MSC immunomodulatory properties following an appropriate period of post-thaw culture suggests that the immediate post-thaw secretory profile should not be misinterpreted as representative of the long-term therapeutic potential of the cellular product [7, 26].

The prominent elevation of pro-inflammatory cytokines in our study provides crucial, complementary insights into post-thaw operational dynamics. Rather than experiencing a generalized metabolic shutdown, the cryopreserved cells demonstrated a selective functional redirection. Quantitatively, the fact that secreted TNF-α levels underwent a dramatic 2.12-fold increase and IL-6 production rose significantly by 1.59-fold post-thaw outlines an acute cellular adaptation to cryogenic shock. Mechanistically, TNF-α operates as a central driver of inflammatory cascades capable of autocrine modification of stem cell behavior, whereas IL-6 functions as a classic pleiotropic cytokine that participates in both pro-inflammatory signaling and tissue regeneration depending on localized concentrations and microenvironmental signals [27, 28]. Crucially, this temporary translational upsurge reflects a metabolic adaptation to freeze – thaw stress rather than a permanent phenotypic conversion toward a classically pro-inflammatory lineage.

This paracrine shift is further characterized by a significant, synchronized suppression of vital angiogenic and trophic factors. Our data revealed that post-thaw VEGF and HGF protein levels dropped significantly by 20.23 % and 15.87 %, respectively, relative to the highly active baseline controls. Both VEGF and HGF serve as vital orchestrators of tissue repair, vascular remodeling, and host cell survival within the MSC secretome [29, 30]. This measurable post-thaw reduction mathematically confirms that cryogenic stress temporarily impairs the immediate regenerative identity of the cells, which carries substantial therapeutic relevance when cryopreserved cellular products are intended for immediate post-thaw clinical applications relying heavily on paracrine-mediated tissue regeneration.

The sharp divergence in secretory kinetics – where specific trophic and anti-inflammatory molecules significantly decline while pro-inflammatory triggers concurrently double – substantiates that the freeze–thaw process alters the programmatic pattern of secretion itself, rather than inducing a non-specific reduction in total cellular metabolic output [31, 32]. Nevertheless, these secretory alterations must be interpreted with caution due to the high inherent variability of mesenchymal stem cell preparations. Phenotypic fluctuations in the post-thaw secretome are heavily dictated by baseline cell density, passage number, tissue source, cryoprotectant concentrations, and the precise window of post-thaw analysis [31]. Consequently, the observed functional disruption reflects an immediate, temporary disturbance in the programmatic signaling balance between immunoregulatory, inflammatory, and trophic factor networks before full cellular stabilization is achieved [10].

Several limitations of the current investigation must be acknowledged. First, this research was executed strictly under *in vitro* conditions; consequently, the documented molecular and secretory kinetics may vary within an *in vivo* physiological microenvironment. Second, while this study provided a comprehensive evaluation of central immunomodulatory, apoptotic, and secretory biomarkers,

it did not evaluate cell migration behavior, multi-lineage differentiation potential, or post-thaw histopathological changes. Finally, the experimental matrix was restricted to a single standard cryopreservation protocol and cooling rate with a single thawing cycle, highlighting the necessity for future expanding evaluations across diverse cryoprotective conditions.

Conclusions

The present comparative study demonstrates that while standard cryopreservation and thawing protocols successfully maintain rat bone marrow-derived mesenchymal stem cell viability safely above critical limits (87.32±2.91 %; P<0.001), the acute thermodynamic stress induces a transient phenotypic and molecular reprogramming of the cellular product immediately post-thaw. At the genomic tier, cryogenic processing triggers a synchronized operational depression of the immunomodulatory machinery, characterized by a statistically significant downregulation of the vital transcripts *Il10* (to 0.68±0.07), *Tgfβ1* (to 0.77±0.06), and *Ido1* (to 0.61±0.06) (P≤0.05). Concurrently, at the translational level, this functional suppression is directly confirmed by a 21.58 % and 21.87 % reduction in secreted IL-10 and TGF-β protein concentrations (P≤0.05), combined with an approximate 15 % to 20 % loss in the paracrine therapeutic secretion of the vital trophic and angiogenic factors VEGF and HGF (P≤0.01). Furthermore, the immediate post-thaw state is marked by an acute intracellular shock that shifts the genomic equilibrium toward mitochondrial-driven apoptotic pathways, resulting in a prominent 1.61-fold upsurge in pro-apoptotic *Bax* and a 1.49-fold increase in executioner *Casp3* expression, running parallel to a significant 30.0 % reduction in protective *Bcl2* mRNA levels (P≤0.05). This molecular stress is accompanied by a dramatic functional reprogramming of the MSC secretome toward an inflammatory phenotype, where secreted TNF-α and IL-6 protein levels prominently escalate by 2.12-fold and 1.59-fold, respectively (P≤0.05).

DECLARATIONS

Ethical Statement

The author declares that this study was conducted using commercially available primary cell lines and strictly did not involve any direct interventions, surgical manipulations, or experimental protocols on live animals. The primary rat bone marrow mesenchymal stem cells (Rattus norvegicus BM-MSCs) utilized in the current research matrix were officially sourced from an authorized commercial vendor (Cell Biologics Company, USA); consequently, obtaining formal institutional bioethics committee approval was not required for this investigation.

Funding

This research received no external funding.

Conflict of Interest

The author declares no conflicts of interest.

Acknowledgements

The author expresses sincere gratitude to everyone who contributed to this research and supported the completion of this study.

Declaration of AI and AI-assisted technologies

The author declares that AI-assisted technologies were utilized solely to assist with linguistic editing, structural formatting, and the refinement of specific manuscript paragraphs. Artificial intelligence technologies were strictly not employed for the generation, rendering, or formatting of scientific data plots, nor for any statistical analyses or interpretation of the biological results. The author maintains full accountability for the integrity of the content, data accuracy, and final conclusions presented in this study.

References

1. Law, S., & Chaudhuri, S. (2013). Mesenchymal stem cell and regenerative medicine: regeneration versus immunomodulatory challenges. *American Journal of Stem Cells*, 2(1), 22–38.
2. Han, X., Liao, R., Li, X., Zhang, C., Huo, S., Qin, L., Xiong, Y., He, T., Xiao, G., & Zhang, T. (2025). Mesenchymal stem cells in treating human diseases: molecular mechanisms and clinical studies. *Signal Transduction and Targeted Therapy*, 10(1), 262. https://doi.org/10.1038/s41392-025-02313-9
3. Esmael, G. K., Rebai, T., & Al-Nailey, K. G. C. (2023). Immunomodulatory effects of bone marrow-derived mesenchymal stem cells on BALB/c mice model with induced systemic lupus erythematosus (SLE): effects of bone marrow-derived mesenchymal stem cells. *Cellular and Molecular Biology*, 69(1), 19–24. https://doi.org/10.14715/cmb/2022.69.1.4
4. Song, N., Scholtemeijer, M., & Shah, K. (2020). Mesenchymal stem cell immunomodulation: mechanisms and therapeutic potential. *Trends in Pharmacological Sciences*, 41(9), 653–664. https://doi.org/10.1016/j.tips.2020.06.009
5. Wang, J., & Li, R. (2024). Correction: Effects, methods and limits of the cryopreservation on mesenchymal stem cells. *Stem Cell Research & Therapy*, 15(1), 372. https://doi.org/10.1186/s13287-024-04001-x
6. Wang, Y., Yang, K., Yuan, S., Huo, F., Yang, C., & Tian, W. (2026). Research advances in cryopreserved preparations of mesenchymal stem cells: technical innovations, application challenges, and quality control. *Frontiers in Bioengineering and Biotechnology*, 14, 1717539. https://doi.org/10.3389/fbioe.2026.1717539
7. Antebi, B., Asher, A. M., Rodriguez, L. A., Moore, R. K., Mohammadipoor, A., & Cancio, L. C. (2019). Cryopreserved mesenchymal stem cells regain functional potency following a 24-h acclimation period. *Journal of Translational Medicine*, 17(1), 297. https://doi.org/10.1186/s12967-019-2038-5
8. Tan, Y., Salkhordeh, M., Wang, J.-P., McRae, A., Souza-Moreira, L., McIntyre, L., Stewart, D. J., & Mei, S. H. J. (2019). Thawed mesenchymal stem cell product shows comparable immunomodulatory potency to cultured cells in vitro and in polymicrobial septic animals. *Scientific Reports*, 9(1), 18078. https://doi.org/10.1038/s41598-019-54462-x
9. Clarke, D. M., Yadock, D. J., Nicoud, I. B., Mathew, A. J., & Heimfeld, S. (2009). Improved post-thaw recovery of peripheral blood stem/progenitor cells using a novel intracellular-like cryopreservation solution. *Cytotherapy*, 11(4), 472–479. https://doi.org/10.1080/14653240902887242
10. Bahsoun, S., Coopman, K., & Akam, E. C. (2020). Quantitative assessment of the impact of cryopreservation on human bone marrow-derived mesenchymal stem cells: up to 24 h post-thaw and beyond. *Stem Cell Research & Therapy*, 11(1), 540. https://doi.org/10.1186/s13287-020-02054-2
11. Ray, S. S., Pramanik, K., Sarangi, S. K., & Jain, N. (2016). Serum-free non-toxic freezing solution for cryopreservation of human adipose tissue-derived mesenchymal stem cells. *Biotechnology Letters*, 38(8), 1397–1404. https://doi.org/10.1007/s10529-016-2111-6

12. Mamo, T., Cox, C. A., Demorest, C., Fontaine, M. J., Hubel, A., Kelley, L., Khan, A., Marks, D. C., Pati, S., Reems, J.-A., Spohn, G., Schäfer, R., Shi, R., Shao, L., Stroncek, D., & McKenna, D. H. (2024). Cryopreservation of mesenchymal stem/stromal cells using a DMSO-free solution is comparable to DMSO-containing cryoprotectants: results of an international multicenter PACT/BEST collaborative study. *Cytotherapy*, 26(12), 1522–1531. https://doi.org/10.1016/j.jcyt.2024.07.001
13. Putra, I., Shen, X., Anwar, K. N., Rabiee, B., Samaeekia, R., Almazyad, E., Giri, P., Jabbehdari, S., Hayat, M. R., Elhusseiny, A. M., Ghassemi, M., Mahmud, N., Edward, D. P., Joslin, C. E., Rosenblatt, M. I., Dana, R., Eslani, M., Hematti, P., & Djalilian, A. R. (2021). Preclinical evaluation of the safety and efficacy of cryopreserved bone marrow mesenchymal stromal cells for corneal repair. *Translational Vision Science & Technology*, 10(10), 3. https://doi.org/10.1167/tvst.10.10.3
14. Shah, F. S., Li, J., Zanata, F., Curley, J. L., Martin, E. C., Wu, X., Dietrich, M., Devireddy, R. V., Wade, J. W., & Gimble, J. M. (2016). The relative functionality of freshly isolated and cryopreserved human adipose-derived stromal/stem cells. *Cells Tissues Organs*, 201(6), 436–444. https://doi.org/10.1159/000446494
15. Xu, X., Liu, Y., Cui, Z., Wei, Y., & Zhang, L. (2012). Effects of osmotic and cold shock on adherent human mesenchymal stem cells during cryopreservation. *Journal of Biotechnology*, 162(2-3), 224–231. https://doi.org/10.1016/j.jbiotec.2012.09.004
16. Shivakumar, S. B., Bharti, D., Jang, S.-J., Hwang, S.-C., Park, J.-K., Shin, J.-K., Byun, J.-H., Park, B.-W., & Rho, G.-J. (2015). Cryopreservation of human Wharton's jelly-derived mesenchymal stem cells following controlled rate freezing protocol using different cryoprotectants; a comparative study. *International Journal of Stem Cells*, 8(2), 155–169. https://doi.org/10.15283/ijsc.2015.8.2.155
17. Ryan, J. M., Barry, F., Murphy, J. M., & Mahon, B. P. (2007). Interferon-γ does not break, but promotes the immunosuppressive capacity of adult human mesenchymal stem cells. *Clinical and Experimental Immunology*, 149(2), 353–363. https://doi.org/10.1111/j.1365-2249.2007.03422.x
18. Holan, V., Hermankova, B., Bohacova, P., Kossl, J., Chudickova, M., Hajkova, M., Krulova, M., Zajicova, A., & Javorkova, E. (2016). Distinct immunoregulatory mechanisms in mesenchymal stem cells: role of the cytokine environment. *Stem Cell Reviews and Reports*, 12(6), 654–663. https://doi.org/10.1007/s12015-016-9688-y
19. François, M., Copland, I. B., Yuan, S., Romieu-Mourez, R., Waller, E. K., & Galipeau, J. (2012). Cryopreserved mesenchymal stromal cells display impaired immunosuppressive properties as a result of heat-shock response and impaired interferon-γ licensing. *Cytotherapy*, 14(2), 147–152. https://doi.org/10.3109/14653249.2011.623691
20. Moll, G., Alm, J. J., Davies, L. C., von Bahr, L., Heldring, N., Stenbeck-Funke, L., Hamad, O. A., Hinsch, R., Ignatowicz, L., Locke, M., Lönnies, H., Lambris, J. D., Teramura, Y., Nilsson-Ekdahl, K., Nilsson, B., & Le Blanc, K. (2014). Do cryopreserved mesenchymal stromal cells display impaired immunomodulatory and therapeutic properties? *Stem Cells*, 32(9), 2430–2442. https://doi.org/10.1002/stem.1729
21. Nasef, A., Chapel, A., Mazurier, C., Bouchet, S., Lopez, M., Mathieu, N., Sensebé, L., Zhang, Y., Gorin, N.-C., Thierry, D., & Fouillard, L. (2006). Identification of IL-10 and TGF-β transcripts involved in the inhibition of T-lymphocyte proliferation during cell contact with human mesenchymal stem cells. *Gene Expression*, 13(4), 217–226. https://doi.org/10.3727/000000006780666957
22. Zhao, Z.-G., Li, W.-M., Chen, Z.-C., You, Y., & Zou, P. (2008). Hematopoiesis capacity, immunomodulatory effect and ex vivo expansion potential of mesenchymal stem cells are not impaired by cryopreservation. *Cancer Investigation*, 26(4), 391–400. https://doi.org/10.1080/07357900701788049
23. Bissoyi, A., & Pramanik, K. (2014). Role of the apoptosis pathway in cryopreservation-induced cell death in mesenchymal stem cells derived from umbilical cord blood. *Biopreservation and Biobanking*, 12(4), 246–254. https://doi.org/10.1089/bio.2014.0005
24. Moll, G., Geißler, S., Catar, R., Ignatowicz, L., Hoogduijn, M. J., Strunk, D., Bieback, K., & Ringdén, O. (2016). Cryopreserved or fresh mesenchymal stromal cells: only a matter of taste or key to unleash the full clinical potential of MSC therapy? In K. Bieback, D. Strunk, & G. Geißler (Eds.), *Mesenchymal stromal cells: analytical and technical advancements* (pp. 77–98). Springer. https://doi.org/10.1007/978-3-319-45457-3_7
25. Aabling, R. R., Alstrup, T., Kjær, E. M., Poulsen, K. J., Pedersen, J. O., Revenfeld, A. L., Møller, B. K., & Eijken, M. (2023). Reconstitution and post-thaw storage of cryopreserved human mesenchymal stromal cells: Pitfalls and optimizations for clinically compatible formulants. *Regenerative Therapy*, 23, 67–75. https://doi.org/10.1016/j.reth.2023.03.006
26. Linkova, D. D., Rubtsova, Y. P., & Egorikhina, M. N. (2022). Cryostorage of mesenchymal stem cells and biomedical cell-based products. *Cells*, 11(17), 2691. https://doi.org/10.3390/cells11172691
27. Li, W., Liu, Q., Shi, J., Xu, X., & Xu, J. (2023). The role of TNF-α in the fate regulation and functional reprogramming of mesenchymal stem cells in an inflammatory microenvironment. *Frontiers in Immunology*, 14, 1074863. https://doi.org/10.3389/fimmu.2023.1074863
28. Majumdar, M. K., Thiede, M. A., Haynesworth, S. E., Bruder, S. P., & Gerson, S. L. (2000). Human marrow-derived mesenchymal stem cells (MSCs) express hematopoietic cytokines and support long-term hematopoiesis when differentiated toward stromal and osteogenic lineages. *Journal of Hematotherapy & Stem Cell Research*, 9(6), 841–848. https://doi.org/10.1089/152581600750062264
29. Hemeda, H., Jakob, M., Ludwig, A.-K., Giebel, B., Lang, S., & Brandau, S. (2010). Interferon-γ and tumor necrosis factor-α differentially affect cytokine expression and migration properties of mesenchymal stem cells. *Stem Cells and Development*, 19(5), 693–706. https://doi.org/10.1089/scd.2009.0365
30. González-González, A., García-Sánchez, D., Dotta, M., Rodríguez-Rey, J. C., & Pérez-Campo, F. M. (2020). Mesenchymal stem cells secretome: The cornerstone of cell-free regenerative medicine. *World Journal of Stem Cells*, 12(12), 1529–1552. https://doi.org/10.4252/wjsc.v12.i12.1529
31. Kehl, D., Generali, M., Mallone, A., Heller, M., Uldry, A.-C., Cheng, P., Gantenbein, B., Hoerstrup, S. P., & Weber, B. (2019). Proteomic analysis of human mesenchymal stromal cell secretomes: a systematic comparison of the angiogenic potential. *npj Regenerative Medicine*, 4(1), 8. https://doi.org/10.1038/s41536-019-0070-y
32. Hsiao, S. T.-F., Asgari, A., Lokmic, Z., Sinclair, R., Dusting, G. J., Lim, S. Y., & Dilley, R. J. (2012). Comparative analysis of paracrine factor expression in human adult mesenchymal stem cells derived from bone marrow, adipose, and dermal tissue. *Stem Cells and Development*, 21(12), 2189–2203. https://doi.org/10.1089/scd.2011.0674

ORCID
G. K. Esmael https://orcid.org/0000-0002-1712-9084